Investigating the role of surface treated titanium dioxide nanoparticles on self-cleaning behavior of an acrylic facade coating

S. Pazokifard, M. Esfandeh, S. M. Mirabedini, M. Mohseni, Z. Ranjbar

Abstract In this study, the addition of silane treated TiO_2 nanoparticles on the self-cleaning properties of an acrylic facade coating was evaluated. Tetraethoxyorthosilicate, TEOS, was used for surface treatment of TiO_2 nanoparticles. The silica grafting on the TiO_2 nanoparticles was characterized via Fourier Transform Infrared spectroscopy, specific surface area measurement, pore size distribution, and real density measurements. The effect of surface treatment and content of nanoparticles on the photocatalytic activity of acrylic coating and self-cleaning properties was studied. For this purpose, the photodegradation of Rhodamine B (Rh.B) dyestuff, as a colorant model, was investigated by colorimetric technique, while the coating samples were exposed to UVA irradiation. Performance of the acrylic coating films was evaluated by gloss change during accelerated weathering conditions. Also, the surface morphology of the coating films was studied using SEM analysis. The results showed that the addition of both treated and untreated TiO_2 nanoparticles provides self-cleaning property to the acrylic coatings. However, silica surface treatment of TiO_2 nanoparticles reduces the coating degradation caused by TiO_2. This is more evident when higher concentrations of the treated TiO_2 nanoparticles are used.

Keywords TiO_2 nanoparticle, Photocatalytic, Self-cleaning, Color coordinate, Coating

S. Pazokifard, S. M. Mirabedini
Colour, Resin & Surface Coatings Department, Iran
Polymer and Petrochemical Institute, P.O. Box 14965-115,
Tehran, Iran

S. Pazokifard
e-mail: s.pazokifard@ippi.ac.ir

S. M. Mirabedini
e-mail: sm.mirabedini@ippi.ac.ir

M. Esfandeh (✉)
Composites & Adhesives Department, Iran Polymer and
Petrochemical Institute, P.O. Box 14965-115, Tehran, Iran
e-mail: m.esfandeh@ippi.ac.ir

M. Mohseni
Department of Polymer Engineering and Color Technology,
Amirkabir University of Technology, P.O. Box 15875-4413,
Tehran, Iran
e-mail: mmohseni@aut.ac.ir

Z. Ranjbar
Department of Surface Coatings & Corrosion, Institute
for Color Science and Technology, P.O. Box 16765-654,
Tehran, Iran
e-mail: ranjbar@icrc.ac.ir

Introduction

In recent years, self-cleaning coatings have been given considerable attention both in industry and academia. Mechanisms and various applications of this type of coating have been well reported in the literature.[1–6] Most of the self-cleaning coatings contain photocatalytic titanium dioxide and are required to be illuminated under an ultraviolet (UV) light source. TiO_2 absorbs light having energy equal to or greater than its band gap energy. During illumination, electrons in TiO_2 are excited from the valence band (VB) to the conduction band (CB).[7,8] Therefore, regions of positive charge (h^+) in form of holes in the VB and a free electron in the CB are created. These charge carriers can either recombine or migrate to the surface. The holes can react with the adsorbed water molecules or with the hydroxyl groups on the surface and produce hydroxyl radicals ($^•OH$). The electrons can combine with atmospheric oxygen and produce superoxide radicals ($OO^•$). These photoinduced radicals are powerful oxidizing species and can deteriorate adsorbed organic contaminants on the particle surface. TiO_2

particles have shown super hydrophilic behavior and, as a result of the "water sheathing effect,"[9,10] the contaminants can be washed away when the external surfaces are exposed to the water flow. These lead to cleaning of the surface by converting the organic molecules to carbon dioxide and water molecules.

Incorporation of photocatalytic TiO_2 particles into or deposited on the surface of organic coatings has many limitations, due to the degradation power of photocatalytic TiO_2 particles on organic media.[10,11] Photocatalytic activity of TiO_2 particles can be adjusted by surface treatment.[12,13] Some reports have cited the increase of photoactivity of TiO_2 as a result of surface modification,[14–18] while others reported a decreasing effect.[19–22]

Because of the aforementioned limitations in the application of TiO_2 in organic media, a few articles have been published on utilizing photocatalytic TiO_2 particles in organic coatings.[23–28] However, if their photocatalytic activity is controlled, they can be an appropriate candidate for self-cleaning acrylic coatings. In this study, the application of silica treated TiO_2 nanoparticles in acrylic facade coatings with the aim of achieving a self-cleaning property is investigated. For this purpose, the commercial TiO_2 nanoparticles were treated by TEOS via a sol–gel process and then incorporated into an acrylic facade coating in different amounts. The photocatalytic activity of the treated TiO_2 into the coating bulk and also the self-cleaning property on the coating surface were studied and compared to that of untreated nanoparticles. Weathering performance of the coatings was also investigated.

Experimental

Materials

TiO_2 nanoparticles, Aeroxide P25, with an average particle size of 30 nm, was obtained from Evonik Industries (Degussa GmbH). It consists of a mixture of 15–30% rutile and 70–85% anatase. Tetraethylorthosilicate, TEOS (>99%), was supplied by Sigma-Aldrich Co. Ethanol (99.9%) and ammonium hydroxide (28%) were purchased from Merck. Acrylic emulsion resin, Mowilith LDM 7717, with 46 wt% solid content, was obtained from Celanese Emulsions Co. Rhodamine B (Rh.B) dyestuff, used as a colorant model, and Texanol (2,2,4-trimethyl-1,3-pentanediol monoisobutyrate), the coalescing agent, were obtained from Ciba-Geigy Ltd. and Eastman Chemical Co., respectively.

Silanization of TiO_2 nanoparticles

TiO_2 nanoparticles were treated with TEOS, through hydrolysis of silane and its condensation with TiO_2 in alkaline media.[20,29,30] For this purpose, 1.5 g of TiO_2 was dispersed in 33 mL ethanol via sonication for 10 min on a Bandelin, HD3200, sonicator (KE-76 probe, pulsation mode of 0.7 s on and 0.3 s off, 70 W power). Ammonium hydroxide was added to adjust pH of the dispersion in the range of 10–11. A certain amount of TEOS (0.25, 0.75, or 3.0 mL), calculated using equation (1),[31] was added gradually to the dispersion during 5 min, while sonicating. The corresponding modified nanoparticles were then coded as 1TT, 3TT, and 12TT, respectively. In sample coding, the number represents weight ratio of TEOS compared to the minimum weight used of TEOS and TT stands for treated TiO_2 nanoparticles.

$$W_{TEOS} = (3 \times S_{P25} \times W_{P25} \times M_{TEOS} \\ \times \text{No. of OH groups} \times 10^{18})/N_A \tag{1}$$

where W_{TEOS} and M_{TEOS} are mass (g) and molecular weight (208.33 g/mol) of TEOS, respectively. W_{P25} and S_{P25} represent mass weight (g) and surface area (50 m²/g) of TiO_2. The number of OH groups for TiO_2 particle is normally about 8–10 OH groups/nm².[32] 10^{18} nm²/m² is a conversion factor and N_A is the Avogadro's number (6.023×10^{23}).

Dispersion was then transferred to a plastic tube—to avoid nucleation on the glass wall—and stirred gently using a magnetic stirrer for 18 h in dark. Finally, it was centrifuged (7000 rpm) and the residue was washed with ethanol and centrifuged again. The washing procedure was repeated five times and the remaining precipitate was dried at 50°C for 48 h.

Surface characterization of the treated TiO_2

Various techniques were employed to evaluate the TEOS grafting on the TiO_2 nanoparticles. Fourier Transform Infrared (FTIR) spectroscopy was carried out with KBr pellet on a Bruker EQUINOX 55 FTIR spectrometer, collecting 16 scans in the 400–4000 cm⁻¹ range at 4 cm⁻¹ resolution. Specific surface area of the powder was measured by nitrogen adsorption according to Brunauer, Emmett, and Teller (BET) analysis. Furthermore, pore size distribution of nanoparticles was calculated using the Barrett–Joyner–Halenda (BJH) method via the Halsey's equation.[33] Samples were conditioned at 120°C for 2 h prior to testing and then adsorption/desorption isotherms were determined using a Quantachrome NOVA 2200 porosimeter at −196°C. Real density of nanoparticles was also determined by displacement method using a Helium pycnometer (Micrometrics, AccuPyc 1330). Three replicates were tested and the average was reported. Based on the characterization results, 12TT nanoparticles were selected for further evaluations in this work.

Preparation of acrylic coatings

Coating samples were formulated by adding different amounts of either treated or untreated TiO_2 nanoparticles

Table 1: Composition of various acrylic coatings, ingredients added to the mixture of resin (30 g) and coalescent agent (0.9 g)

Sample coding	P25 (g)	12TT (g)	0.25 g L^{-1} Rh.B solution (g)	Distilled water (g)
R	–	–	–	25.0
R-Rh.B	–	–	25.0	–
U-0.5-C	0.069	–	25.0	–
U-0.5-W	0.069	–	–	25.0
U-1-C	0.138	–	25.0	–
U-1-W	0.138	–	–	25.0
U-1.5-C	0.207	–	25.0	–
U-1.5-W	0.207	–	–	25.0
U-2-C	0.276	–	25.0	–
U-2-W	0.276	–	–	25.0
T-0.5-C	–	0.069	25.0	–
T-0.5-W	–	0.069	–	25.0
T-1-C	–	0.138	25.0	–
T-1-W	–	0.138	–	25.0
T-2-C	–	0.276	25.0	–
T-2-W	–	0.276	–	25.0
T-2.5-C	–	0.345	25.0	–
T-2.5-W	–	0.345	–	25.0

The letters in the first column correspond to: Contains Rhodamine (C), No Rhodamine (W), Resin (R), Treated TiO$_2$ (T), Untreated TiO$_2$ (U), and the number shows wt% of TiO$_2$ nanoparticles based on the solid content of resin in the formulations

to 25 g Rh.B solution (0.25 g L^{-1}) and dispersed by sonicating for 10 min. The dispersions were then added gradually to a mixture of 30 g acrylic resin and 0.9 g Texanol, and mixed thoroughly using a magnetic stirrer for 30 min. Coating samples with a wet film thickness of 200 ± 10 μm were then applied on the float glass and aluminum plates, using a film applicator (Elcometer Doctor Applicator). The applied films were then allowed to dry at ambient temperature (25 ± 2°C) for 24 h.

A similar procedure was used to prepare coatings for the evaluation of the self-cleaning property. However, in these coatings only distilled water (free of Rh.B) was used as the dispersion media and an aqueous solution of Rh.B (0.1 g L^{-1}) was applied on the surface of the dried coating and then left to dry in a dark chamber at ambient temperature for 24 h. The formulations used for the preparation of acrylic coatings are listed in Table 1.

Dispersion of TiO$_2$ nanoparticles in the coatings

To investigate the dispersion status of untreated and silica treated TiO$_2$ nanoparticles in acrylic films; SEM analysis were performed using a Cambridge Stereo scan S360 electron microscope. The freestanding films

were prepared by applying the coating formulation on a prewaxed glass plate with a wet film thickness of 200 ± 10 μm. The film was dried at ambient temperature for 24 h and then placed in a distilled water bath for about 15 min, to facilitate its removal from the glass surface. Finally, it was left to dry at room temperature for 24 h. SEM micrographs were taken from the cryogenically fractured cross section of the coatings in liquid nitrogen as well as the coating surface. The sample was sputter coated with a thin layer (∼10 nm) of gold and examined using the scanning electron microscope operated in the secondary electron mode at 10 kV.

Colorimetric study of Rh.B degradation

Degradation of Rh.B in both coating bulk and on the surface of the coating was evaluated via color coordinates data measurements using a Gretag Macbeth Color-Eye 7000A spectrophotometer, before and after exposure to the UVA irradiation. Total color change (ΔE) was calculated from Commission International de l'e′ clairage (CIE) ($L*a*b*$)1976, D65/10°, formula according to equation (2).[34]

$$\Delta E^* = \sqrt{(\Delta L^*)^2 + (\Delta a^*)^2 + (\Delta b^*)^2} \tag{2}$$

where L^* represents the brightness or gray value and varies between 100 (white) and 0 (black); $a*$ (red-green) and $b*$ (yellow-blue) are the chromaticity coordinates.

To evaluate the degradation of Rh.B and in the other words the photocatalytic activity of TiO$_2$ nanoparticles in the acrylic coatings, the coating samples were exposed to the UVA irradiation (340 nm, 0.89 W m^{-2}) in a Q-Panel accelerated weathering chamber (Q-Panel QUV/Spray) at 60°C and different time intervals for 270 min. Three replicates were placed in a QUV chamber and an unexposed sample was also used as the "standard". The photocatalytic decomposition of Rh.B was monitored by measuring color coordinates values ($L*$, $a*$, and $b*$). Rh.B degradation was determined using a quantitative parameter, "Degradation Factor, D.F." which is defined according to equation (3):

$$D.F. (\%) = \left(\frac{\Delta E_t}{\Delta E_{max}}\right) \times 100 \tag{3}$$

where ΔE_t is the color difference between the UVA exposed sample for a given time and the corresponding standard sample, and ΔE_{max} shows the maximum color difference between the coatings with and without Rh.B, at a certain amount of TiO$_2$ nanoparticles.

Rh.B degradation on the surface of the coating can be regarded as a measure of the self-cleaning property on the surface of the coating. To evaluate the self-cleaning property of the coatings containing various

amounts of TiO$_2$ nanoparticles (treated and untreated), color change of the coating was measured during exposure to UVA irradiation using an OSRAM ULTRA-VITALUX® (300 W) irradiation source which simulates natural sunlight.[35] The lamp was placed at about 80 cm above the samples and the test was performed at 30°C over 20 h. Color coordinates prior to UV exposure were used as the standard in calculation of ΔE.

Durability of the coatings

Effect of accelerated weathering conditions on the surface properties of the acrylic films containing various wt% of TiO$_2$ nanoparticles was studied using SEM analysis and gloss measurement. For this purpose, an accelerated weathering test was conducted in the QUV chamber according to ASTM D 4587 standard practice, for about 540 h. According to the test procedure, the specimens were alternately exposed to UVA irradiation (340 nm, 0.89 W m^{-2}) at 60°C for 8 h and followed by 4 h of water condensation at 45°C periodically. Gloss of the coating films was measured by a Glossmeter (Nova gloss) in 20°, according to ASTM D 523 test practice, before and during UVA exposure in the QUV chamber.

The changes in the surface morphology of the coatings after exposure to accelerated weathering conditions were evaluated using SEM analysis. The surface preparation for the analysis was as explained in section "Dispersion of TiO$_2$ nanoparticles in the coatings".

Results and discussion

The performance of TiO$_2$ nanoparticles in a polymeric matrix is highly affected by surface chemistry and loading of nanoparticles. The surface chemistry determines the hydrophobic/hydrophilic behavior, which is directly affected by surface functional groups on the surface of the nanoparticles. This in turn, implies the dispersability of the particles into the polymeric matrix and hence the possible particle loading. The surface characteristics of the nanoparticles also influence the photocatalytic activity as well as self-cleaning behavior of the nanoparticles on the coating surface. Thus, surface characterization of the treated and untreated TiO$_2$ nanoparticles seems quite necessary in order to have a better understanding of their role in the coating.

Characterization of silica treated TiO$_2$ nanoparticles

Figure 1 shows the FTIR spectra of treated and untreated TiO$_2$ nanoparticles as well as TEOS. The
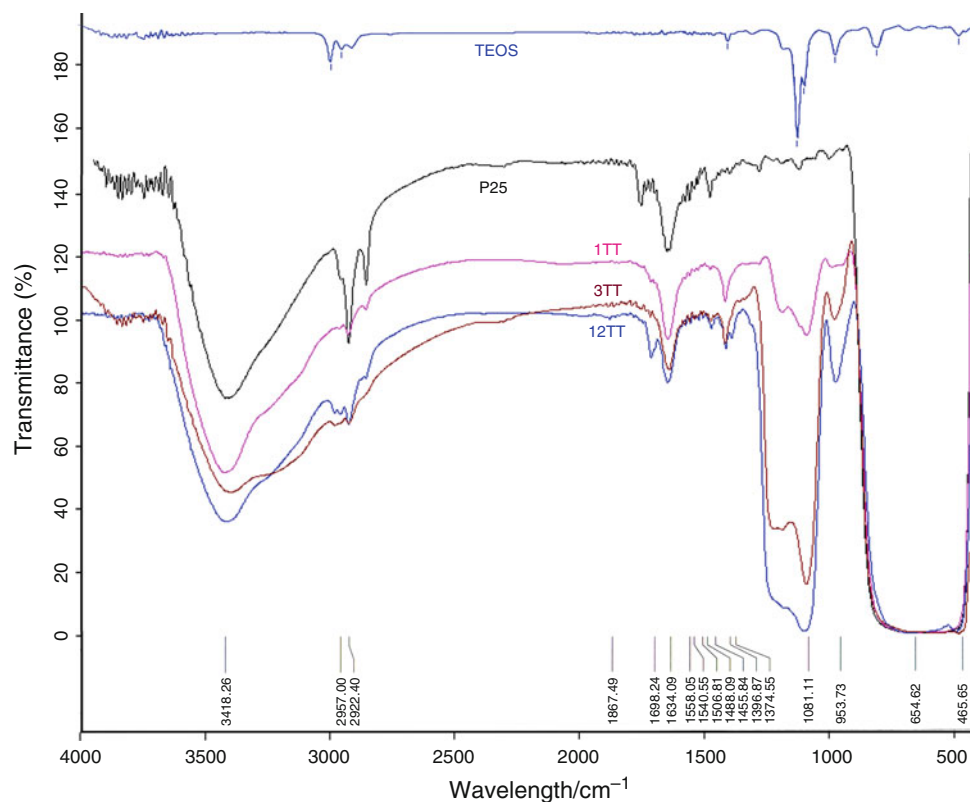

Fig. 1: FTIR spectra of TEOS, untreated (P25) and treated TiO$_2$ with different amounts of TEOS (1TT, 3TT, and 12TT)

spectra related to TiO_2 nanoparticles were normalized with respect to the peak in the range of 800–500 cm^{-1}. The broad band at around 3400 cm^{-1} and the sharp band at 1616 cm^{-1}, observed in both untreated and treated TiO_2 nanoparticles, are attributed to the water adsorbed by nanoparticles.[20] Major absorptions at about 1081, 953, and 465 cm^{-1} represent the characteristic bonds of Si–O-Si asymmetric stretching, Ti–O–Si asymmetric stretching and Ti–O stretching, respectively.[36–41] According to the literature,[39,42] Ti–O–Si and Si–OH bands appear at around 955 and 935 cm^{-1}, respectively. However, in the case of Si–OH another absorption band must also appear at 3745 cm^{-1},[39,42] which is not observed in this case. Thus, the band which appeared at 953 cm^{-1} is assigned to Ti–O–Si and confirms grafting on the surface of TiO_2 nanoparticles.

In the spectra of the treated nanoparticles, a doublet peak appears in the region 1040–1187 cm^{-1}, showing an increase in the intensity with increasing TEOS content. This can be related to self-condensation of TEOS on the surface of silica treated TiO_2 nanopartricles. It is believed that self-condensation of TEOS mainly happens on the surface of TiO_2 nanoparticles, because silane has already been grafted to the surface of TiO_2 nanoparticles. A suggested schematic of TEOS grafted TiO_2 nanoparticles is shown in Fig. 2.

Specific surface area, average pore volume, and pore diameter are among the structural parameters of particles and can be used to characterize the status of a grafted layer on its surface. The results for specific surface area (determined by BET method), pore

Fig. 2: Schematic of TEOS treated TiO_2 nanoparticles

characteristics, i.e., volume and diameter (determined by BJH method) and real density of untreated and silica treated TiO_2 nanoparticles are summarized in Table 2. The increase observed in the specific surface area and also pore's volume for silica treated TiO_2 nanoparticles can be considered as the indication of silica grafting on the surface of the particle.

Surface porosity consists of micropores (pore diameter less than 2 nm) and mesopores (pore diameter between 2 and 10 nm) can be determined by gas sorption. BET, as the most well known gas sorption model, is applied to obtain the specific surface area of microporous materials, although from a scientific point of view the assumptions made in the BET theory do not take into account macropore filling. By definition, macropores are too large to show up as pores within the experimental data range.[43] Surface treatment may provide a porous layer on the surface through grafting. It is believed that grafting on the surface makes it somehow irregular and rougher and obviously this leads to an increase in the specific surface area. Generally, the average surface area of untreated titania pigment is 6–9 m^2/g. However, because of the increased surface roughness, the inorganic coatings may double the pigment surface area when compared to that reported for untreated pigment.[44,45]

The BET results indicate that increasing the amount of TEOS to about a stoichiometric value increases the specific surface area. This can be attributed to the fact that surface grafting can increase the surface roughness and the rough surfaces, e.g., inorganic coatings, have much more specific surface area than the smooth surfaces. Thus, increasing in BET values from 65.95 to 79.23 m^2 g^{-1} (neat nanoparticles to 1TT), may be regarded as an indication of silica grafting. With further increase in TEOS level in treatment process, from 3TT to 12TT, the amount of surface area is rapidly increased from 96.06 to 132.96 m^2 g^{-1}. The increase in surface area after silane treatment can be partly due to self-condensation of TEOS molecules, but this is more likely to happen at higher concentrations (e.g., 12TT). In other words, with increasing TEOS content in the surface treatment process, the chances for separate hydrolysis and self-condensation of silica particles may be increased. However, the appearance of Ti–O–Si absorption bond in FTIR
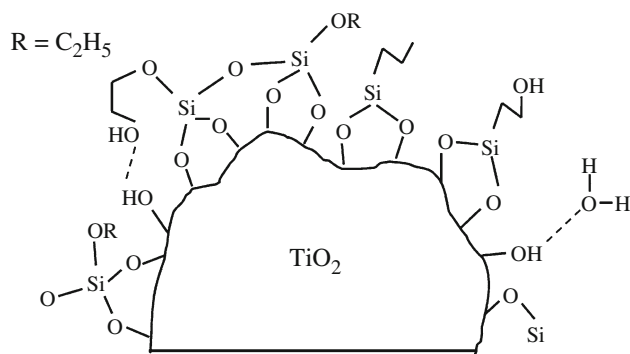
Table 2: Specific surface area, porosity data, and real density of untreated and different silica treated TiO_2 nanoparticles

Sample coding[a]	P25	1TT	3TT	12TT
BET: Single point (m^2 g^{-1})	65.95	77.83	94.45	132.90
BET: Multi point (m^2 g^{-1})	66.68	79.23	96.06	134.96
Desorption pore volume BJH (cm^3 g^{-1})	0.15	0.21	0.21	0.23
Desorption pore diameter BJH (Å)	21.41	23.96	21.34	10.07
Real density (g cm^{-3})	0.04 ± 3.72	0.01 ± 3.71	0.02 ± 3.40	0.02 ± 2.81

[a] The numbers show the weight coefficient of TEOS in treatment reactions and TT stands for the treated samples

analysis, even at high TEOS concentration confirms the grafting of TEOS onto the TiO_2 nanoparticles.

There is also an increase in the average pore volume of the treated nanoparticles; however, a further increase in TEOS content would not change the situation. The increase in pore volume can be related to the condensation reaction of silanol groups and formation of siloxane linkages on the surface of TiO_2 which increases the porosity of the silica layer on the surface of TiO_2 nanoparticles. The corresponding data for pore diameter in 12TT sample (i.e., 10.07 Å) reveal a significant decrease with the addition of TEOS. The smaller pore diameter (about 10 Å) in the adsorbed silica layer of 12TT in comparison with the other samples (about 21 Å), can be considered as a sign for dense character of the surface layer in the treated TiO_2 nanoparticles. This can be the result of the formation of a relatively denser grafting layer, which mainly happens at around stoichiometric values of the ingredients and thereby affects the silica surface morphology. Considering the real density value for silica (ca. 2.20 g cm^{-3}),[46] the decrease observed in the real density of the treated TiO_2 (Table 2) can also be considered as further evidence for silica grafting.

Dispersion of nanoparticles in the coating

SEM micrographs of the cross section and surface of the coatings containing 1 and 2 wt% of untreated and silica treated nanoparticles are illustrated in Fig. 3. Nonuniform distribution of untreated nanoparticles in the form of relatively large particle aggregates is observed in both bulk and on the surface of the coating film. This is due to colloidal instability of the dispersion and tendency of the nanoparticles to form agglomerate during film formation. This is more evident at higher nanoparticles' loading, i.e., 2 wt%. Silica treatment alters the dispersion behavior of TiO_2 nanoparticles, as it reduces the aggregates size and enhances the homogeneity of particles distribution.

Photocatalytic activity studies

Photocatalytic activity of TiO_2 in acrylic water-based coatings containing various levels of untreated and treated nanoparticles was determined using discoloration monitoring of Rh.B within the coating samples. The calculated average color differences at a given time, ΔE_t, are shown in Fig. 4. As it can be observed, Rh.B dyestuff in absence of TiO_2 nanoparticles slightly degrades with value of $\Delta E_t = 12.6$ after 270 min UVA irradiation exposure time. This can be assigned to the reaction in presence of oxygen which includes the following possible steps[47]:

$$RB + h\nu \rightarrow RB^* \tag{4}$$

$$RB^* + O_2 \rightarrow RB^{+\bullet} + O_2^{-\bullet} \tag{5}$$

$$O_2^{-\bullet} + H^+ \rightarrow OOH^\bullet \tag{6}$$

$$RB^{+\bullet} \xrightarrow{O_2} Rhodamine \rightarrow Products \tag{7}$$

Also, the presence of both untreated (Fig. 4a) and treated (Fig. 4b) nanoparticles has a significant effect on the coating's discoloration during UVA irradiation. In all cases, with increasing nanoparticles' loading ΔE_t is increased; however, it reaches an almost steady state after about 1.5 h irradiation. Also, an increase in the initial slope of the curves with the addition of nanoparticles is observed, indicating the higher degradation rate of Rh.B at higher loadings. For the coatings containing untreated nanoparticles (Fig. 4a), $\Delta E_t = 22.8$ ($t = 270$ min) was obtained with the addition of 1.5 wt% nanoparticles and beyond which ΔE_t variations were not significant, probably due to difficulty in dispersion and also colloidal instability. It is believed that untreated nanoparticles tend to adhere together (Fig. 3), due to their surface characteristics. Thus, less effective surface area is available for the adsorption of Rh.B, which is necessary for the initial step of photocatalytic/photo-degradation process. In coatings containing treated nanoparticles, silica surface treatment of TiO_2 leads to a better and more stable dispersion of the nanoparticles (Fig. 3), which enhances the effective surface area for Rh.B adsorption. Also, higher percentages of the treated nanoparticles can be incorporated into the coating which enhances ΔE_t, so that $\Delta E_t = 24.7$ ($t = 270$ min) was obtained at 2.5 wt% loading.

For quantitative determination of Rh.B degradation, the degradation factor (D.F. %) was calculated according to equation (3). For this purpose, ΔE_t at different UVA irradiation exposure times was normalized by dividing it to the ΔE_{max}. ΔE_{max} was defined as the maximum color difference for each coating sample containing Rh.B compared with its sample counterpart without Rh.B, as shown in Table 3. The plots of normalized ΔE vs UVA irradiation time are shown in Fig. 5. The trend of color changes in the coatings is similar to that shown in Fig. 4; however, the loading limitations are much better illustrated, particularly for the coatings containing treated nanoparticles (Fig. 5b). The critical loading was found to be 1.5 and 2.5 wt% for untreated and treated nanoparticles, respectively.

In Table 4, D.F. % for various coatings after 270 min exposure to UVA irradiation and also photocatalytic activity as the result of TiO_2 presence in the coatings are listed. It is worth mentioning that the overall color changes observed in the coatings originated from photolysis of Rh.B itself and the degradation caused by photocatalytic activity of TiO_2. Equation (8) can be used to quantify the effect of TiO_2 photoactivity in the coating.

Photocatalytic activity of TiO_2 (%)

$$= \left(\frac{D.F._S - D.F._R}{D.F._R} \right) \times 100 \tag{8}$$

Poor dispersion   Good dispersion
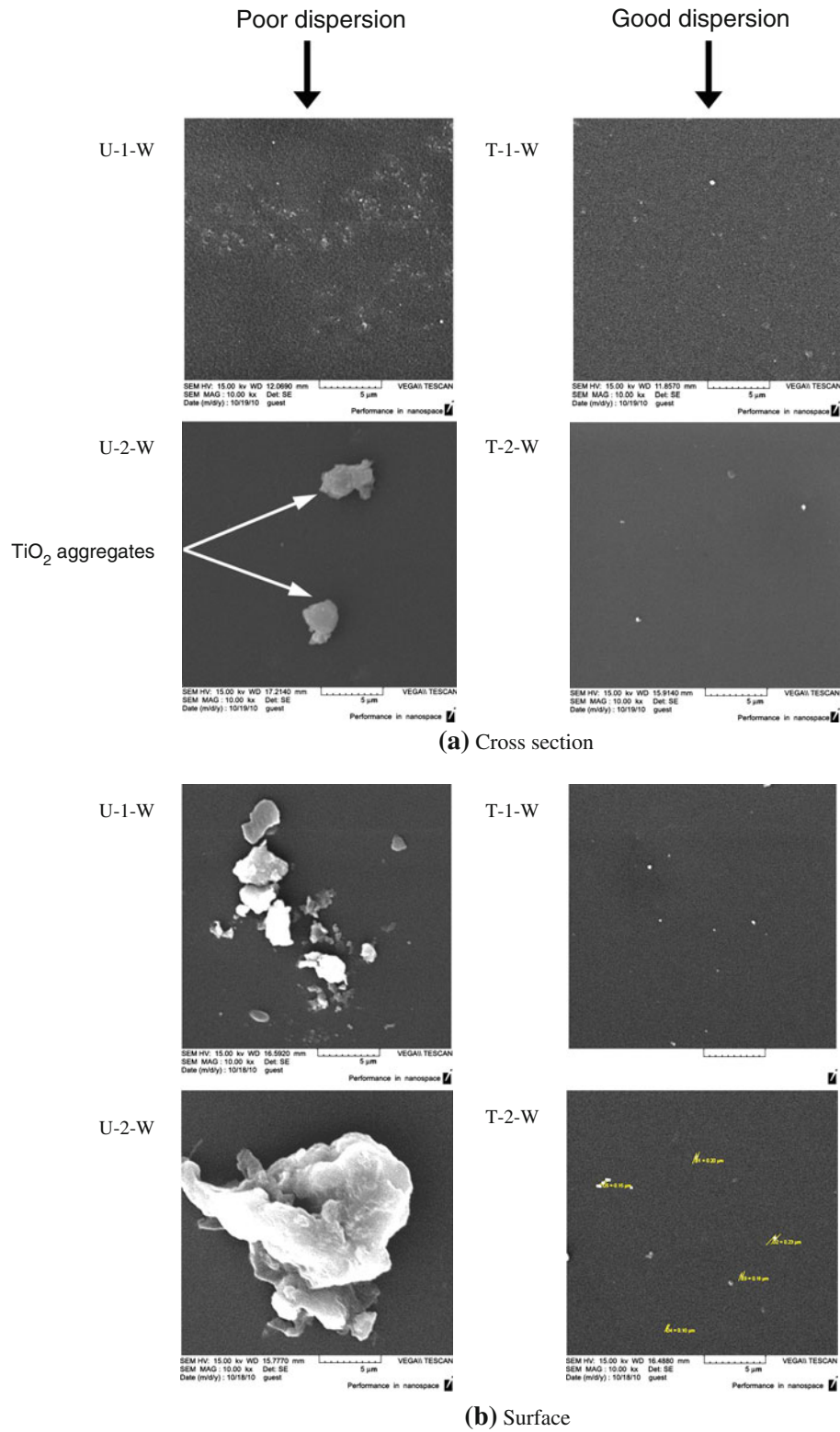

(a) Cross section

(b) Surface

Fig. 3: SEM micrographs of (a) cross section and (b) surface of acrylic coatings containing 1 and 2 wt% of untreated (P25) and silica treated TiO$_2$ (12TT) nanoparticles (×5000)
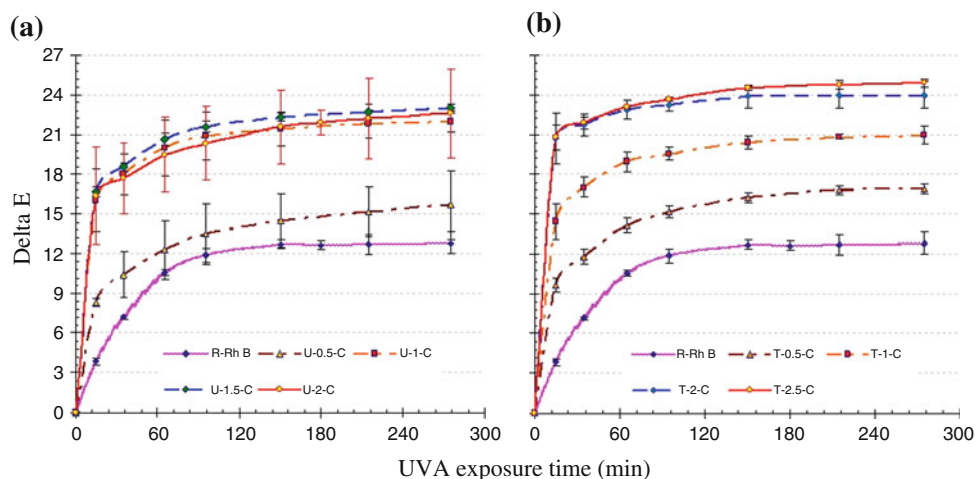
Fig. 4: Color difference, ΔE_t, of the acrylic films containing various amount of (a) untreated and (b) silica treated TiO$_2$ nanoparticles in the presence of Rh.B, during UVA exposure times

Table 3: ΔE_{max} measurement results for coating samples

Row	Sample coding	L^*	a^*	b^*	ΔE_{max}
1	R	87.48	1.28	−13.71	18.65
	R-RhB	78.61	15.39	−22.07	
2	U-0.5-W	77.67	1.00	−7.02	21.04
	U-0.5-C	72.41	19.16	−16.25	
3	U-1-W	81.43	1.48	−3.64	23.11
	U-1-C	72.77	21.08	−12.31	
4	U-1.5-W	78.79	1.41	−1.96	26.25
	U-1.5-C	69.36	23.25	−13.04	
5	U-2-W	77.65	1.35	−2.38	28.09
	U-2-C	68.93	26.18	−12.22	
6	T-0.5-W	86.95	1.40	−7.11	20.49
	T-0.5-C	78.41	18.08	−15.40	
7	T-1-W	83.81	1.39	−4.51	21.11
	T-1-C	74.13	19.36	−9.86	
8	T-2-W	78.65	1.49	−0.90	21.18
	T-2-C	69.83	20.12	−5.78	
9	T-2.5-W	76.32	1.52	−0.28	22.60
	T-2.5-C	67.38	21.77	−4.81	

where D.F.$_S$ is the degradation factor of the sample containing TiO$_2$ nanoparticles and Rh.B, and D.F.$_R$ is the degradation factor of the coating which only contains Rh.B.

From Table 4, it is concluded that both "content" and "surface treatment" of nanoparticles affect Rh.B degradation. Also, in the coating's bulk and at equal concentrations, silica treated nanoparticles have higher photodegradation activity than their untreated counterparts. This is particularly true at higher concentrations of nanoparticles, e.g., 2 wt% where a photocatalytic activity of 44.5% is achieved. This can

be again attributed to better dispersion and improved stability of silica treated nanoparticles in water-based acrylic emulsion during film formation and drying. On the other hand, better dispersion causes less light scattering and greater light transmission and absorption. As light absorption is an important factor in photocatalytic activity of particles, the improved photocatalytic activity can thus be explained.

Self-cleaning property

In this study Rhodamine B (Xantane dye with an anthracene moiety) is used as a pollutant model and its photocatalytic decomposition under UVA radiation is assessed through discoloration measurements.[48] Anthracene moiety of Rodamine B makes it suitable as a PAHs model. PAHs or polycyclic aromatic hydrocarbons are among the soiling agents found in urban environments and are generally found in oil, coal, and tar deposits. They are produced as the by-products of fuel burning.[49] Discoloration of Rh.B on the coating shows photoactivity at the surface, which could be a stand in for self-cleaning ability.

Variations of ΔE vs UVA exposure time for different coatings are illustrated in Fig. 6. For TiO$_2$-free coating, the color difference is very small and is attributed to Rh.B and the coating degradation itself, under UVA irradiation.

With the addition of TiO$_2$ nanoparticles to the coating an increase in ΔE is observed which is higher for untreated TiO$_2$. This is in such a way that with the addition of 1 and 2 wt% of TiO$_2$, ΔE values for untreated nanoparticles are 2.3 and 6.8 compared to 1.3 and 4.3 for their treated counterparts, respectively. From these results it is understood that at equal concentrations the untreated nanoparticles are more effective than the treated one in giving the self-cleaning property. Presumably this is due to enhanced
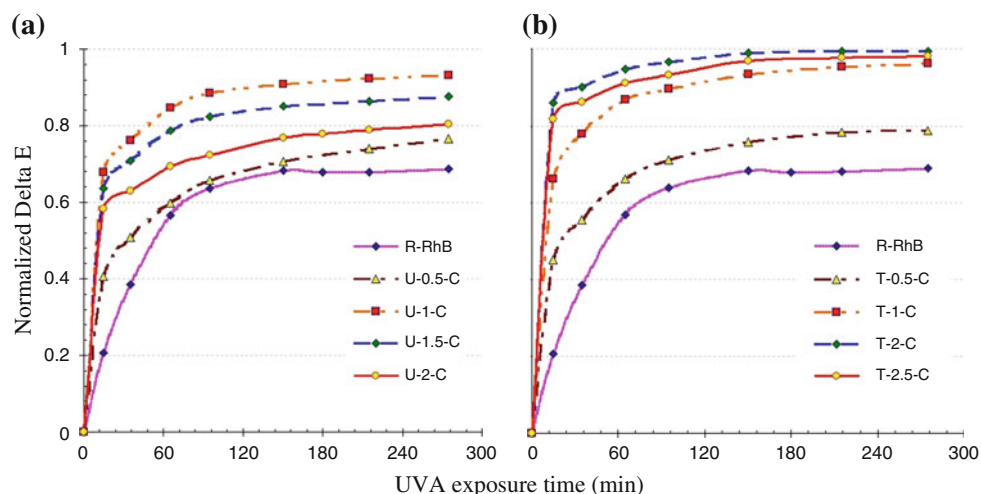
Fig. 5: Normalized ΔE_t of coating films containing various amounts of (a) P25 and (b) 12TT nanoparticles in the presence of Rh.B, during UVA irradiation time

Table 4: Rh.B degradation factor and photocatalytic activity in the acrylic coatings containing various wt% nanoparticles, after exposure to 270 min UVA radiation

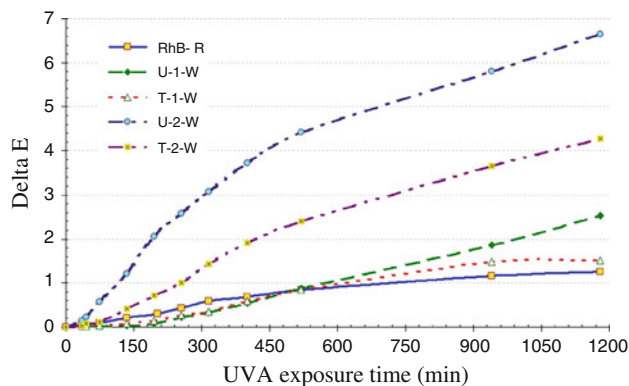| Sample coding	D.F. (%)	Photocatalytic activity (%)
R-RhB	68.8	0
U-0.5-C	76.5	11.2
U-1-C	93.2	35.5
U-1.5-C	87.6	27.3
U-2-C	80.4	16.9
T-0.5-C	78.9	14.7
T-1-C	96.1	39.7
T-2-C	99.4	44.5
T-2.5-C	99.4	44.5

Fig. 6: Color difference induced by discoloration of RhB deposited on the surface of various acrylic films exposed to UVA irradiation

photoactivity of untreated TiO_2 nanoparticles caused by more active sites on the particle's surface as compared to the treated TiO_2 and also the fact that untreated nanoparticles are poorly dispersed.[50,51] Because of the colloidal instability, they tend to migrate to the coating surface rather than remaining in the coating's bulk, in contrast to what happens for the treated nanoparticles. Therefore, the surface becomes TiO_2-rich and hence more degradation of the pollutant occurs. This may also be achieved by increasing the concentration of the treated nanoparticles, however, longer time will be needed to get the self-cleaning property and if the concentration is not adequate (e.g. 1 wt%) it may not even happen at all.

For better illustration of the effect of surface treatment of TiO_2 nanoparticles on self-cleaning property, the Relative Photocatalytic Activity, RPA, is defined as equation (9)[20]:

$$RPA\ (\%) = 100 \times \Delta E_T / \Delta E_U \qquad (9)$$

where ΔE_T and ΔE_U represent color difference of acrylic coatings containing treated and untreated TiO_2 nanoparticles, respectively. According to equation (9) the coatings containing 1 and 2 wt% of treated nanoparticles have an RPA 56.5% (1.3/2.3) and 63.2% (4.3/6.8), respectively. It appears that with increasing the concentration of the treated nanoparticles their degradation effect is increased but still is less than the untreated.

Eventually, it can be concluded that addition of TiO_2 nanoparticles (untreated and silica treated) into the acrylic facade coatings in adequate amounts provides self-cleaning property. Also, it can be stated that ''loading levels'' and ''surface chemistry'' of TiO_2 nanoparticles affects the self-cleaning property of the acrylic facade coatings.
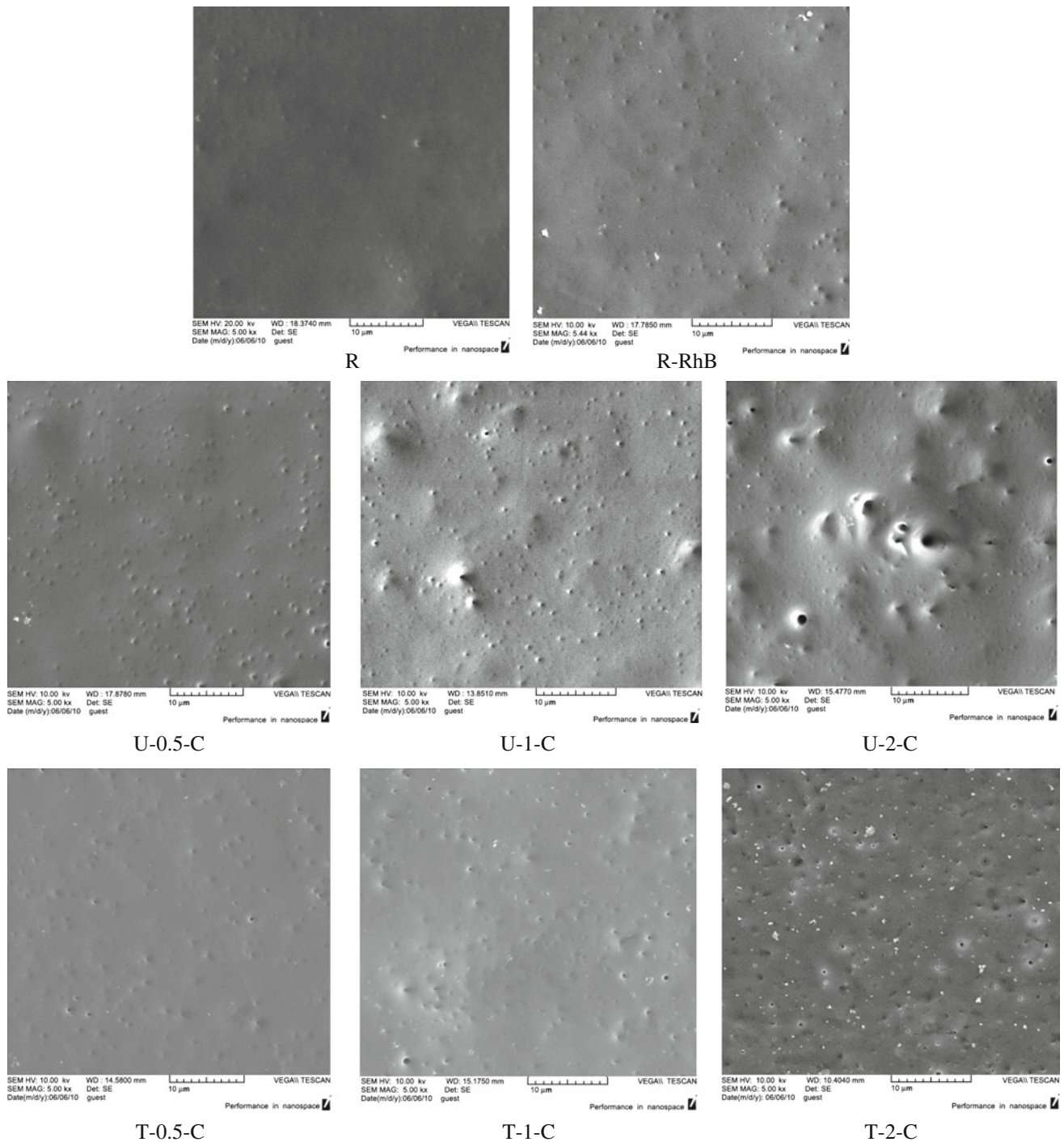
Fig. 7: SEM micrographs of different acrylic coating films exposed to accelerated weathering conditions (170 h in Q-Panel)

Coating durability

SEM micrographs of acrylic films containing different wt% of TiO_2 nanoparticles after 170 h exposure to accelerated weathering conditions are shown in Fig. 7. As it is clear, the neat acrylic coating (R) reveals a relatively proper weathering performance with no detectable defect on the surface. Coating containing

Rh.B dyestuff (R-Rh.B) shows lower resistance against weathering conditions compared with neat coating. Some holes and spots are observed on the surface of the coating sample after weathering which are related to photodegradation activity of dyestuff itself. Addition of untreated nanoparticles reduces the coating performance and with further increasing the concentration of nanoparticles to 2 wt% the situation
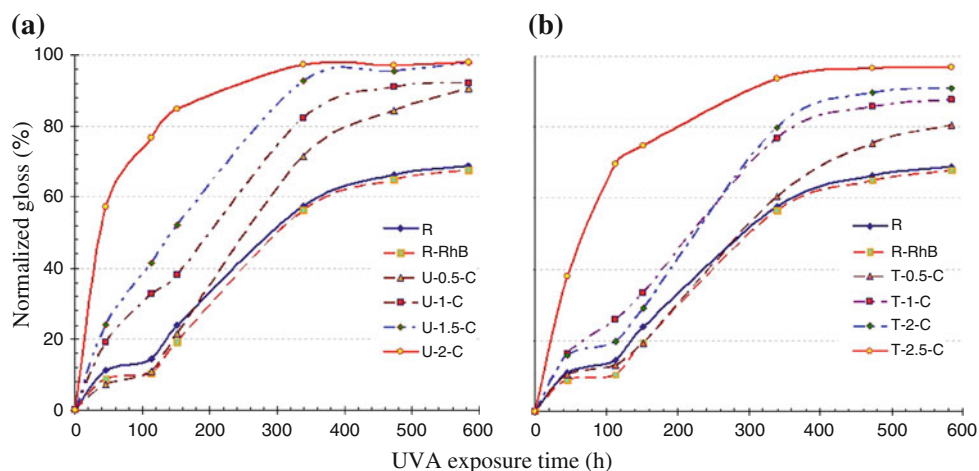
(a) **(b)**

Fig. 8: Normalized gloss (loss of gloss) of different acrylic coating films containing various levels of nanoparticles, during exposure to UVA irradiation conditions

becomes even worse so that severe defects in form of big and deep holes appear throughout the surface (U-2-C). This indicates the high photocatalytic activity of untreated TiO_2 nanoparticles. With the addition of treated nanoparticles, the degradation in the coating is still somehow observable but to a much lower extent (T-2-C). This can be attributed to lower photocatalytic effect and better dispersion of silica treated TiO_2 nanoparticles in the coating. The decrease in photocatalytic activity of TiO_2 as the result of surface treatment, which leads to a better performance of the coating, is more evident at higher nanoparticles' loadings.

Gloss is an appearance property that is very important for many coatings.[52] It is affected by the coating substrate and both the thickness and evenness of the coating itself. Gloss measurements quantify the amount of light reflected from the object's surface at the specular angle. Degradation usually leads to poor gloss owing to diffuse light scattering. The total gloss loss after weathering is often a good indication of coating performance as well as a guide to perceived appearance.[53] The results for gloss measurement of the coating samples containing various levels of nanoparticles and exposed to UVA irradiation are shown in Fig. 8. The results show that at zero-time exposure with the addition of both treated and untreated TiO_2 nanoparticles the gloss of the coating is reduced. The more evident reduction for the untreated nanoparticles is due to the formation of agglomerates on the surface of the coating, which makes the surface rough and scatters the light. Obviously, with increasing the nanoparticles' loading the gloss of the surface is further reduced. At equal concentrations of nanoparticles, the coatings containing treated nanoparticles show less gloss loss and lower rate of gloss reduction during accelerated weathering, as compared to untreated nanoparticles. From these results it can be supposed that silica grafting of nanoparticles rather improves gloss retention of acrylic

coating film compared with untreated nanoparticles. The results obtained for the gloss measurements of the coatings containing treated and untreated nanoparticles are in agreement with the results of photocatalytic effect and morphological studies.

Conclusions

TiO_2 nanoparticles were surface treated by TEOS and characterized with various techniques. The role of surface treated TiO_2 nanoparticles on self-cleaning behavior of an acrylic facade coating was investigated. In surface treatment of TiO_2 in alkaline media a dense layer of silica is formed on its surface around the stoichiometric values.

SEM analysis confirmed that the silica treated nanoparticles have a better dispersion in the coating and form smaller aggregates compared with their untreated counterparts. Colorimetric measurements showed that the presence of TiO_2 nanoparticles promotes the degradation of Rh.B, the pollutant model, in the acrylic coating. The treated TiO_2 is less photoactive than the untreated, but the treated particles may retain enough photoactivity to be useful as self-cleaning coatings. SEM analysis and gloss measurements proved that the coatings containing treated TiO_2 nanoparticles have a better durability than those having untreated ones. In other words, the treated nanoparticles are less photoactive, but improved dispersion helps the bulk properties. Considering the requirements for the self-cleaning property and coating's durability, loading level and surface chemistry of TiO_2 nanoparticles are the two determining factors to obtain the optimum coating performance. Eventually, it can be concluded that addition of adequate amounts of silica treated TiO_2 nanoparticles (e.g., 2 wt%) into the acrylic coatings provides a self-cleaning property in acrylic facade coatings.

References

1. Nun, E, Oles, M, Schleich, B, "Lotus Effect-Surfaces." *Macromol. Symp.*, **187** 677–682 (2002)

2. Blossey, R, "Self-Cleaning Surfaces—Virtual Realities." *Nat. Mater.*, **2** 301–306 (2003)

3. Parkin, I, Palgrave, R, "Self-Cleaning Coatings." *J. Mater. Chem.*, **15** 1689–1695 (2005)

4. Ma, M, Hill, R, "Superhydrophobic Surfaces." *Curr. Opin. Colloid Interface Sci.*, **11** 193–202 (2006)

5. Zhang, X, Shi, F, Niu, J, Jiang, Y, Wang, Z, "Superhydrophobic Surfaces: From Structural Control to Functional Application." *J. Mater. Chem.*, **18** 621–633 (2008)

6. Hochmannova, L, Vytrasova, J, "Photocatalytic and Antimicrobial Effects of Interior Paints." *Prog. Org. Coat.*, **67** 1–5 (2010)

7. Fujishima, A, Hashimoto, K, Watanabe, T, *TiO_2 Photocatalysis: Fundamental and Applications*. BKC, Tokyo, 1999

8. Winkler, J, *Titanium Dioxide*. Vincentz, Hannover, 2003

9. Fujishima, A, Rao, TN, Tryk, DA, "Titanium Dioxide Photocatalysis." *J. Photochem. Photobiol., C*, **1** (1) 1–21 (2000)

10. Ghosh, S, *Functional Coatings: By Polymer Microencapsulation*. Wiley-VCH Verlag Gmbh, Germany, 2006

11. Braun, JH, "Titanium Dioxide's Contribution to the Durability of Paint Films." *Prog. Org. Coat.*, **15** 249–260 (1987)

12. Fujishima, A, Zhang, X, Tryk, D, "TiO_2 Photocatalysis and Related Surface Phenomena." *Surf. Sci. Rep.*, **63** 515–582 (2008)

13. Górska, P, Zaleska, A, Kowalska, E, Klimczuk, T, Sobczak, J, Skwarek, E, Janusz, W, Hupka, J, "TiO_2 Photoactivity in Vis and UV Light: The Influence of Temperature and Surface Properties." *Appl. Catal., B*, **84** 440–447 (2008)

14. Damchan, J, Sikong, L, Kooptarnond, K, Niyomwas, S, "Contact Angle of Glass Substrate with TiO_2/SiO_2 Thin Film." *J. Nat. Sci.*, **7** (1) 19–23 (2008)

15. Zhou, M, Yu, J, Cheng, B, "Effects of Fe-doping on the Photocatalytic Activity of Mesoporous TiO_2 Powders Prepared by an Ultrasonic Method." *J. Hazard. Mater.*, **137** 1838–1847 (2006)

16. Vohra, M, Kim, S, Choi, W, "Effects of Surface Fluorination of TiO_2 on the Photocatalytic Degradation of Tetramethylammonium." *J. Photochem. Photobiol., A*, **160** 55–60 (2003)

17. Yang, S, Chen, Y, Zheng, J, Cui, Y, "Enhanced Photocatalytic Activity of TiO_2 by Surface Fluorination in Degradation of Organic Cationic Compound." *J. Environ. Sci. (China)*, **19** (1) 86 (2007)

18. Sikong, L, Kongreong, B, Kantachote, D, Sutthisripok, W, "Photocatalytic Activity and Antibacterial Behavior of Fe^{3+}-Doped TiO_2/SnO_2 Nanoparticles." *Energy Res. J.*, **1** 120–125 (2010)

19. El-Toni, A, Yin, S, Sato, T, "Control of Silica Shell Thickness and Microporosity of Titania–Silica Core–Shell Type Nanoparticles to Depress the Photocatalytic Activity of Titania." *J. Colloid Interface Sci.*, **300** 123–130 (2006)

20. Siddiquey, I, Furusawa, T, Sato, M, Honda, K, Suzuki, N, "Control of the Photocatalytic Activity of TiO_2 Nanoparticles by Silica Coating with Polydiethoxysiloxane." *Dyes Pigment*, **76** 754–759 (2008)

21. Tada, H, Kokubu, A, Iwasaki, M, Ito, S, "Deactivation of the TiO_2 Photocatalyst by Coupling with WO_3 and the Electrochemically Assisted High Photocatalytic Activity of WO_3." *Langmuir*, **20** 4665–4670 (2004)

22. Libanori, R, Giraldi, T, Longo, E, Leite, E, Ribeiro, C, "Effect of TiO_2 Surface Modification in Rhodamine B Photodegradation." *J. Sol-Gel Sci. Technol.*, **49** 95–100 (2009)

23. Nakajima, A, Hashimoto, K, Watanabe, T, Takai, K, Yamauchi, G, Fujishima, A, "Transparent Superhydrophobic Thin Films with Self-Cleaning Properties." *Langmuir*, **16** 7044–7047 (2000)

24. Niegisch, N, Akarsu, M, Csögör, Z, Ehses, M, Schmidt, H, "TiO_2 Nanoparticle Coatings for Self-Cleaning and Antimicrobial Application." *Proceedings of Hygienic Coatings*, Paint Research Association, Brussels, Belgium, paper 20, 2002

25. Yamauchi, G, Riko, Y, Yasuno, Y, Shimizu, T, Funakoshi, N, "Nanostructured Titanium Dioxide Films for Self-Cleaning and Self-Decontaminating Surfaces." *Nano and Hybrid Coatings*, Paint Research Association, Manchester, UK, paper 20, 2005

26. Allen, N, Edge, M, Ortega, A, Liauw, C, Stratton, J, McIntyre, R, "Behavior of Nanoparticle (Ultrafine) Titanium Dioxide Pigments and Stabilisers on the Photooxidative Stability of Water Based Acrylic and Isocyanate Based Acrylic Coatings." *Polym. Degrad. Stab.*, **78** 467–478 (2002)

27. Allen, N, Edge, M, Ortega, A, Sandoval, G, Liauw, C, Verran, J, Stratton, J, McIntyre, R, "Degradation and Stabilisation of Polymers and Coatings: Nano Versus Pigmentary Titania Particles." *Polym. Degrad. Stab.*, **85** 927–946 (2004)

28. Allen, N, Edge, M, Verran, J, Stratton, J, Maltby, J, Bygott, C, "Photocatalytic Titania Based Surfaces: Environmental Benefits." *Polym. Degrad. Stab.*, **93** 1632–1646 (2008)

29. Jaroenworaluck, A, Sunsaneeyametha, W, Kosachan, N, Stevens, R, "Characteristics of Silica Coated TiO_2 and Its UV Absorption for Sunscreen Cosmetic Applications." *Surf. Interface Anal.*, **38** 473–477 (2006)

30. Bechger, L, Koenderink, AF, Villem, LV, "Emission Spectra and Lifetimes of R6G Dye on Silica-Coated Titania Powder." *Langmuir*, **18** 2444–2447 (2002)

31. Sepeur, S, *Nanotechnology: Technical Basics and Applications*. Vincentz Network, Hannover, 2008

32. Somasundaran, P, *Encyclopedia of Surface and Colloid Science*, Vol. 4, p. 2863. Taylor & Francis Group, CRC Press, New York, Boca Raton, 2006

33. Barrett, E, Joyner, L, Halenda, P, "The determination of pore volume and area distributions in porous substances. I. Computations from nitrogen isotherms." *J. Am. Chem. Soc.*, **73** 373–380 (1951)

34. McLaren, K, "XIII—The Development of the CIE 1976 (L* a* b*) Uniform Colour Space and Colour Difference Formula." *J. Soc. Dyers Colour.*, **92** 338–341 (1976)

35. Hidalgo, M, Maicu, M, Navío, J, Colón, G, "Photocatalytic Properties of Surface Modified Platinised TiO_2: Effects of Particle Size and Structural Composition." *Catal. Today*, **129** 43–49 (2007)

36. Dean, JA, *Analytical Chemistry*. McGraw-Hill, New York, 1995

37. Kim, J, Chang, S, Kong, S, Kim, K, Kim, J, Kim, W, "Control of Hydroxyl Group Content in Silica Particle Synthesized by the Sol-Precipitation Process." *Ceram. Int.*, **35** 1015–1019 (2009)

38. Li, Z, Hou, B, Xu, Y, Wu, D, Sun, Y, "Hydrothermal Synthesis, Characterization, and Photocatalytic Performance of Silica-Modified Titanium Dioxide Nanoparticles." *J. Colloid Interface Sci.*, **288** 149–154 (2005)

39. Julian, JM, *An Infrared Spectroscopy Atlas for the Coatings Industry*, 4th ed., Vol. 1. Federation of Societies for Coatings Technology, Pennsylvania, 1991

40. Zhao, Y, Xu, L, Wang, Y, Gao, C, Liu, D, "Preparation of Ti–Si mixed oxides by sol–gel one step hydrolysis." *Catal. Today*, **93** 583–588 (2004)

41. Zeitler, VA, Brown, CA, "The Infrared Spectra of Some Ti–O–Si, Ti–O–Ti and Si–O–Si Compounds." *J. Phys. Chem.*, **61** 1174–1177 (1957)

42. Nakamura, M, Kobayashi, M, Kuzuya, N, Komatsu, T, Mochizuka, T, "Hydrophilic Property of SiO_2/TiO_2 Double Layer Films." *Thin Solid Films*, **502** 121–124 (2006)

43. Condon, JB, *Surface Area and Porosity Determinations by Physisorption: Measurements and Theory*. Elsevier B.V., The Netherlands, 2006

44. Braun, JH, "Titanium Dioxide: A Review." *J. Coat. Technol.*, **69** (868) 59–72 (1997)

45. Farrokhpay, S, "A Review of Polymeric Dispersant Stabilisation of Titanium Pigment." *Adv. Colloid Interface Sci.*, **151** 24–32 (2009)

46. Van Hoang, V, "Molecular Dynamics Simulation of Amorphous SiO_2 Nanoparticles." *J. Phys. Chem. B*, **111** 12649–12656 (2007)

47. Wilhelm, P, Stephan, D, "Photodegradation of Rhodamine B in Aqueous Solution Via $SiO_2@TiO_2$ Nano-spheres." *J. Photochem. Photobiol., A*, **185** 19–25 (2007)

48. Ying, M, Yao, J-N, "Comparison of Photodegradative Rate of Rhodamine B Assisted by Two Kinds of TiO_2 Films." *Chemosphere*, **38** 2407–2414 (1999)

49. Gustafson, KE, Dickhut, RM, "Particle/Gas Concentrations and Distributions of PAHs in the Atmosphere of Southern Chesapeake Bay." *Environ. Sci. Technol.*, **31** 140–147 (1997)

50. Mirabedini, A, Mirabedini, S, Babalou, A, Pazokifard, S, "Synthesis, Characterization and Enhanced Photocatalytic Activity of TiO_2/SiO_2 Nanocomposite in an Aqueous Solution and Acrylic-Based Coatings." *Prog. Org. Coat.*, **72** (3) 453–460 (2011)

51. Pazokifard, S, Mirabedini, S, Esfandeh, M, Mohseni, M, Ranjbar, Z, "Silane Grafting of TiO_2 Nanoparticles: Dispersibility and Photoactivity in Aqueous Solutions." *Surf. Interface Anal.*, **44** 41–47 (2012)

52. Stoye, D, Freitag, W, *Paints, Coatings and Solvents*. Wiley-VCH Verlag Gmbh, Germany, 1998

53. Weldon, DG, *Failure Analysis of Paints and Coatings*. John Wiley & Sons, London, 2009